JOURNAL OF THERMOPHYSICS AND HEAT TRANSFER
Vol. 11, No. 4, October–December 1997

Characterization of Plenum Spectra in an Arcjet Wind Tunnel

Mohammad A. Rob* and Larry H. Mack Jr.†
University of Houston—Clear Lake, Houston, Texas 77058
Sivaram Arepalli‡
G. B. Tech, Inc., Houston, Texas 77058
and
Carl D. Scott§
NASA Johnson Space Center, Houston, Texas 77058

An optical fiber is used to collect radiation from the plenum of an arcjet wind tunnel. Studying the spectra, the electronic excitation temperatures are determined from the Boltzmann plots of atomic oxygen and nitrogen emission lines. In the case of atomic oxygen, the temperature is found to be about 15,000 ± 3400 K, and that of nitrogen is found to be 7600 ± 1500 K. Determination of molecular vibrational–rotational temperature is made by comparing experimental and theoretical spectra of the N_2^+ molecular radiation. The temperature is estimated to be 9700 ± 1200 K, using an integrals ratio method.

Nomenclature

A_{ul} = Einstein transition probability
$B\,^2\Sigma_u^+$ = upper electronic state designation of N_2^+
E_u = excitation energy of upper energy state
g_l = degeneracy factor for lower energy state
g_u = degeneracy factor for upper energy state
k = Boltzmann constant
N_g = population density in the ground energy state
T_e = excitation temperature
v' = upper vibrational level quantum number
v'' = lower vibrational level quantum number
$X\,^2\Sigma g^+$ = ground electronic state designation of N_2^+
Δv = change in vibrational quantum number
λ = wavelength of light

I. Introduction

THERMAL protection system (TPS) materials are used in space vehicles to shield them from the high heating environment encountered during atmospheric re-entry. The TPS materials are tested in arcjet wind tunnels that simulate re-entry conditions. The arcjet is a facility that produces high-enthalpy, high-speed flowfields inside an evacuated chamber by expanding arc-heated air through a conical or channel nozzle. Test materials are placed in the flowfield, and their capabilities are studied over broad ranges of enthalpy and pressure of the flow. How well these tests simulate the actual heating environment encountered by space vehicles depends on the chemical and thermal characteristics of the simulated flow. A large fraction of the heat is in latent form, in energy of dissociation of N_2 and O_2 molecules into N and O atoms. These atoms may recombine on the TPS surface to form molecules and transfer the heat of dissociation to the surface.[1] The rate at which the atoms catalytically recombine on the surface then significantly affects the heat flux to the thermal protection materials. The heat flux therefore depends on the properties of the flow as well as the catalytic properties of the material surface.

Arcjet flows are in chemical and thermal nonequilibrium because of low pressure and high-velocity flows. The flow characterization requires the determination of species concentration, velocity, and energy distribution among various atomic, molecular, and ionic species present in the flow.[2] Measurements of various temperatures such as the translational, electronic excitational, and the molecular rotational and vibrational temperatures are necessary to determine the energy modes. At equilibrium, all temperatures should be the same. Arcjets are typically run with simulated air and closely mimic atmospheric re-entry conditions. The major species in the flow are N_2, O_2, N, O, NO, N_2^+, O_2^+, N^+, O^+, NO^+, and electrons.[3] Concentrations of these species change when the enthalpy and pressure of the flow changes. As enthalpy increases, O_2 dissociation increases, and at higher enthalpies, N_2 also becomes dissociated.

In a typical arcjet flow, the excited gas first enters a settling chamber, termed plenum, where the gas presumably spends sufficient time to form a uniform mixture of its constituents. The gas then expands through a nozzle into a vacuum chamber, where it forms a freestream moving at hypersonic speeds. A complete characterization of the arcjet flow requires characterizations of both the freestream and plenum flows. The pressure in the plenum is of the order of 1 atm. The velocity of the flow is relatively low. The flow in this region may be in thermal equilibrium, but not necessarily in chemical equilibrium. The freestream flow is characterized by chemical and thermal nonequilibrium that arises because of the expansion of the gas through the nozzle, and is often treated as a chemically frozen ideal gas.[4]

Presented as Paper 95-2126 at the AIAA 30th Thermophysics Conference, San Diego, CA, June 19–22, 1995; received Nov. 8, 1996; revision received March 24, 1997; accepted for publication March 24, 1997. Copyright © 1997 by the American Institute of Aeronautics and Astronautics, Inc. No copyright is asserted in the United States under Title 17, U.S. Code. The U.S. Government has a royalty-free license to exercise all rights under the copyright claimed herein for Governmental purposes. All other rights are reserved by the copyright owner.

*Assistant Professor, School of Natural and Applied Sciences, 2700 Bay Area Boulevard; currently Operations Specialist, Lockheed Martin Space Mission Systems and Services, S36-2, 555 Forge River Road, Webster, TX 77598. Member AIAA.

†Graduate Student, School of Natural and Applied Sciences, 2700 Bay Area Boulevard; currently Electro-Optical Engineer, Lockheed Martin Missiles and Space Systems, 3251 Hanover Street, Palo Alto, CA 94304-1191.

‡Principal Engineer, 2200 Space Park Drive, Houston, TX 77058. Senior Member AIAA.

§Research Engineer, M/S ES3, 2101 NASA Road One. Associate Fellow AIAA.

In the past, good progress has been made in understanding the flow characteristics of the freestream and the shock layer.[5–7] However, the starting conditions of the flow, i.e., of the plenum area, are not completely understood.[8,9] The accuracy of the simulated models for the arcjet flow, such as the NATA[10] code (a one-dimensional nonequilibrium nozzle flow code), depends on the knowledge of the initial conditions of the flow. Terrazas-Salinas et al.[9] studied radiation in the arc column of an arcjet. Studying oxygen and nitrogen lines, and the continua, they determined the average temperature of the gas at two locations of the arc column, under four different operating conditions. They have also mentioned that the existing radiation transition probabilities (A values) for nitrogen are not very accurate, in the sense that using these values, a complete calculated spectrum of nitrogen in the 300–900 nm range does not agree with the experimental observation. Comparing the experimental and calculated spectra, Terrazas-Salinas et al.[9] concluded that the flow in the arc column is in thermal equilibrium in the arcjets at NASA Ames Research Center. The arcjets that are used at NASA Johnson Space Center (JSC) have different arc column configurations, and also use larger cone angle (15-deg) nozzles. These differences are expected to result in somewhat different arcjet flows. In the current study,[11] we have investigated the radiation characteristics of the NASA JSC arcjet plenum area by using an optical fiber to collect radiation. Studying atomic oxygen and nitrogen emission lines, we have been able to determine the average electronic excitation temperature. Attempts were also made to determine the molecular vibrational–rotational temperature using N_2^+ molecular spectra. The details of the experimental arrangement and the results are discussed in the following text.

II. Experimental Details

A. Arcjet Wind Tunnel

The experiment was carried out in one of the two test chambers of the arcjet wind-tunnel facility at NASA JSC. A schematic of an arcjet wind tunnel is shown in Fig. 1a. General operating characteristics of the NASA JSC arc heaters and the arcjet flows are given in Ref. 5, and a brief description is given here for the sake of completeness. The arc heater is of the segmented constricted type with a tungsten button cathode at the upstream end, and a conical copper anode at the downstream end. The constrictor column is made up of a number of individually water-cooled, electrically insulated constrictor segments, assembled in modular packs. Depending on the desired test condition, the length of the arc heater can be varied between 30–300 cm. The arc can be operated at powers up to 10 MW. The test gases for air (oxygen and nitrogen mixture) are introduced tangentially at several points along the length of the constrictor column. Argon is used as a starter gas to initiate discharge, but is turned off after the discharge is initiated. The heated gas flows through a small settling chamber (plenum), then through a converging–diverging conical nozzle to a vacuum chamber, where the gas acquires free-flow conditions at supersonic speeds. The enthalpy of the gas can be changed by changing arc current and the mass flow rate of the gas. The arc current can be adjusted between 200–2000 A, and the total gas mass flow rate can be varied between 0.02–0.6 kg/s. Table 1 shows two typical run conditions of the arcjet used in the experiment. As shown in Table 1, in some experiments, the arcjet was run with 100% nitrogen gas.

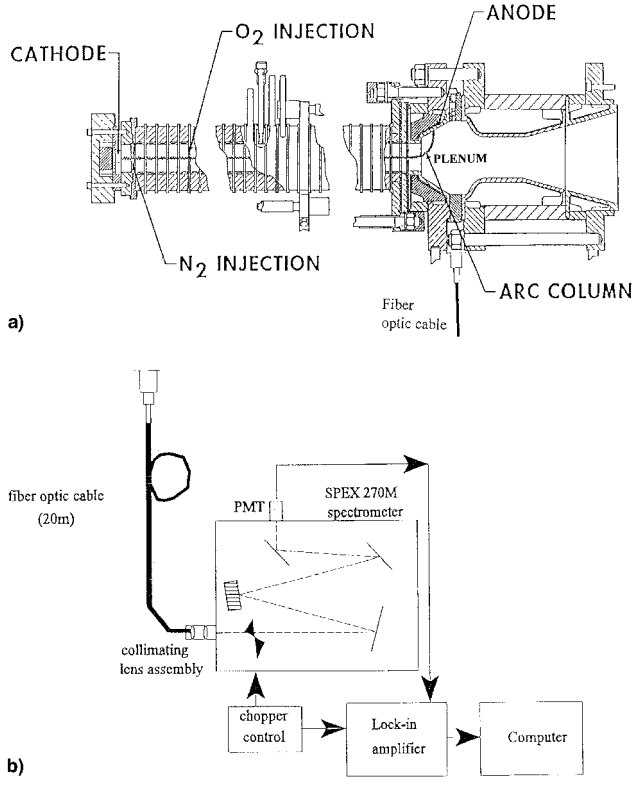

Fig. 1 Schematic of the a) arcjet wind tunnel and b) experimental arrangement for plenum radiation study using an optical fiber.

B. Radiation Measurements

The experimental optical arrangement is shown in Fig. 1b. The radiation was collected from the plenum area using an optical fiber. The fiber was installed in one of the disks of the plenum area through a threaded insert. The fiber insert was a 5-cm-long hollow stainless-steel tube with a quartz window and a gas purging system. The quartz window serves as a vacuum seal holding the gas pressure while transmitting radiation from ultraviolet to near-infrared. The fused silica optical fiber was 20 m long and had a core diameter of 200 μm. It was chosen for its excellent transmission in the 300–900 nm wavelength range.

Radiation collected by the optical fiber is focused into a spectrometer through a collimated lens assembly. Radiation from the exit slit of the spectrometer was collected with a photomultiplier tube (PMT), and the signal from the detector was fed into a lock-in-amplifier (SRS Model 550). A chopper installed inside the spectrometer provided the trigger signal for the lock-in-amplifier. Output from the lock-in-amplifier was collected and the data were stored using data acquisition software (SRS Model 575). The stored data were analyzed and plotted using a commercial software, Sigma-Plot.

Two spectrometers equipped with multiple gratings (combination of 600, 1200, 1800, or 2400 lines/mm) were used in the radiation study. The SPEX 270M is a small spectrometer with a 0.27-m optical path and high throughput. Most of the initial studies were performed with this spectrometer. The SPEX 1877 is a triple spectrometer with an optical path of 0.6 m. The bandwidths of these spectrometers were measured using the yellow doublet of a low-pressure mercury lamp. The bandwidth of the SPEX 270M spectrometer was found to be 0.625 nm, with a 600 lines/mm grating and 100-μm entrance and exit slit widths. With a 1200 lines/mm grating, and entrance and exit slits of 200 μm, the bandwidth of the triplemate

Table 1 Typical run conditions of the arcjet

Run conditions	Low enthalpy	High enthalpy
Arc current, A	450	1000
Arc voltage, V	2400	2300
Total enthalpy, MJ/kg	6.9	13.6
Mass flow rate, kg/s	0.1	0.1
Gas mixture	77% N_2 + 23% O_2 or 100% N_2	——

spectrometer was found to be 0.3 nm. Cutoff filters were used in the spectrometer to block unwanted higher grating-orders of spectral lines.

Once the data were collected, they were corrected for wavelength and intensity response of the instruments. The wavelength calibration of the spectrometer was performed by using a low-pressure mercury source. The intensity calibration for the instrument was performed using a tungsten ribbon filament lamp, whose calibration is traceable to the NIST standard.

III. Results and Discussion

A. Identification of the Emission Lines

Once the radiation was collected, the emission lines were identified by comparing with the standard tables of atomic and molecular spectra,[12,13] and with the theoretical plots of NEQAIR-5 (nonequilibrium air radiation) codes assuming an optically thin gas medium.[14] Most of the emission in the plenum was due to atomic oxygen and nitrogen, and some due to N_2^+ (first negative system) molecular ion. Tables 2 and 3 give atomic oxygen and nitrogen emission lines, respectively, identified from the plenum spectra presented in Fig. 2. The data include spectral lines taken with the SPEX 270M spectrometer using a 600 lines/mm grating, and with the SPEX 1877 spectrometer using a 1200 lines/mm grating. These two spectrometer settings allowed us to collect two spectra in a wide spectral range: the first with a high signal-to-noise ratio, and the second with higher resolution. Tables 2 and 3 also contain some other parameters that are discussed later. Note that most of the emission lines observed in the spectra are because of atomic nitrogen, and there are several multiplets (denoted as M in Tables 2 and 3) in the whole spectrum. The oxygen lines are isolated and the intensity of the unresolved triplet at 777 nm is by far the highest in the spectrum. There is also a broad continuum present in the spectrum. Note also that the measured intensities caused by two different spectrometers under the same operating conditions of the arcjet are very much the same.

Table 2 Atomic nitrogen lines identified from the plenum radiation spectra

λ, A	g_l	g_u	E_u, cm^{-1}	A_{ul}, 10^8/s	I_{600}[a]	I_{1200}[a]
4099.95 (M)[b]	2	4	110,522	0.034	7.2	8.2
4109.96 (M)[b]	4	6	110,546	0.04	11.6	12.2
4151.46	6	4	107,447	0.013	6.6	7.8
4215.92 (M)[b]	2	4	106,998	0.031	3.2	3.8
4223.04 (M)[b]	6	6	107,039	0.051	6.6	7.2
4914.90	2	2	106,479	0.00759	3.5	4.2
4935.03	4	2	106,479	0.0158	10.8	11.5
5281.18 (M)[b]	6	6	107,039	0.00282	6.5	7.2
5328.70 (M)[b]	6	8	106,871	0.00254	13	14
7423.64	2	4	96,752	0.052	160	160
7442.30	4	4	96,752	0.106	300	310
7468.31	6	4	96,752	0.161	420	440
8200.36	2	2	95,477	0.0367	45	45
8210.71	4	4	95,495	0.0363	110	115
8216.32	6	6	95,533	0.16	420	425
8223.12	4	2	95,477	0.202	215	240
8242.37	6	4	95,495	0.102	185	205

[a]Denotes relative intensity collected using 600 or 1200 lines/mm grating.
[b]M denotes multiplets whose line separations are comparable to the bandwidth of the triplemate spectrometer with a 1200 lines/mm grating.

Table 3 Atomic oxygen lines identified from the plenum radiation spectra

λ, A	g_l	g_u	E_u, cm^{-1}	A_{ul}, 10^8/s	I_{600}[a]	I_{1200}[a]
3947.3	5	15	99,095	0.00326	2.6	2.7
4368.3	3	9	99,680	0.0066	6.6	6.6
6157.3	15	25	102,865	0.0701	53	53
6455.0	15	5	102,116	0.071	28	22
7156.8	5	5	116,631	0.473	32.5	33.4
7773.4 (M)[b]	5	15	86,629	0.34	1200	1200
7949.3	15	21	113,719	0.373	40	41.5
8446.5	3	9	88,631	0.28	145	148

[a]Denotes relative intensity collected using 600 or 1200 lines/mm grating.
[b]M denotes multiplets whose line separations are comparable to the bandwidth of the triplemate spectrometer with a 1200 lines/mm grating.

B. Determination of Electronic Excitation Temperature

The relative intensities of the atomic emission lines were used to determine the electronic excitation temperature. In an equilibrium flow, when the gas is optically thin, the intensity I_e of an atomic spectral line is related to T_e and the wavelength emitted by the species[9,15–17]:

$$I_e \propto (A_{ul} g_u/\lambda) N_g \exp(-E_u/kT_e) \tag{1}$$

where A_{ul} is from the upper state to the lower state. It is clear from Eq. (1) that the intensity of an atomic spectral line depends on the parameters A_{ul}, g_u, λ, and E_u of the transition involved. Thus, a plot of $\ell n(\lambda I_e/g_u A_{ul})$ vs E_u (Boltzmann plot) results in a straight line, whose slope is $(-1/kT_e)$, and which gives T_e.

Figure 3 shows Boltzmann plots of atomic oxygen and nitrogen lines for two different scanning conditions of the spectrometers, as mentioned earlier. To obtain an accurate value of the temperature, only the strong and isolated lines in the spectra are used in the plots. Also, as seen in Tables 2 and 3, the measured intensities for a particular spectral line are not very different for the two spectrometers, and all spectral lines are included in the plot. In the case of atomic oxygen, the temperature is found to be about 15,000 ± 3400 K, and that for nitrogen it is about 7600 ± 1500 K. The average electronic excitation temperature as determined is about 11,300 K. The difference between these temperatures is very large, which indicates that there is some error in the temperature determination technique. Terrazas-Salinas et al.[9] speculate that the nitrogen atomic transition probabilities are in error. There is the possibility that the triplets are not totally resolved, nor are they totally combined in the measurements. If we exclude the multiplets in the spectra, we obtain a temperature of about 17,900 ± 3600 for oxygen, and about 13,100 ± 1500 for nitrogen. These temperatures are closer together, and their error bands overlap. The mean of these is 15,500 ± 2800 K. The errors in the temperatures correspond to the standard error in the slope of a least-square fitting of the data in the Boltzmann plot. It should be clear from Fig. 3 that the Boltzmann plots of oxygen span a wider range of excitation energies than that of nitrogen. Also, one notices large scatter in the data points clustered around the excitation energy of about 107,000 cm^{-1}. This results in very large error bars around the mean. In addition, the uncertainty in the existing A values, as noted by Terrazas-Salinas et al.,[9] prompts us to believe that nitrogen data cannot be relied upon. Thus, the temperature determined from the oxygen plots should be a better indicator of the excitation temperature of the arcjet plenum than that determined from the nitrogen plots.

C. Determination of the Vibrational–Rotational Temperature

In principle, one could obtain vibrational–rotational temperatures by using Boltzmann plots of the vibrational–rotational transitions, as in the case of atomic transitions. But molecular vibrational–rotational transitions are complex and far less intense than those of atomic transitions, and are not well resolved in the experimental spectra. The experimental spectra are further complicated because of the overlapping spectra of more than one molecular species, such as NO, N_2, and N_2^+. Thus, different approaches were taken to determine the molecular vibrational–rotational temperature.

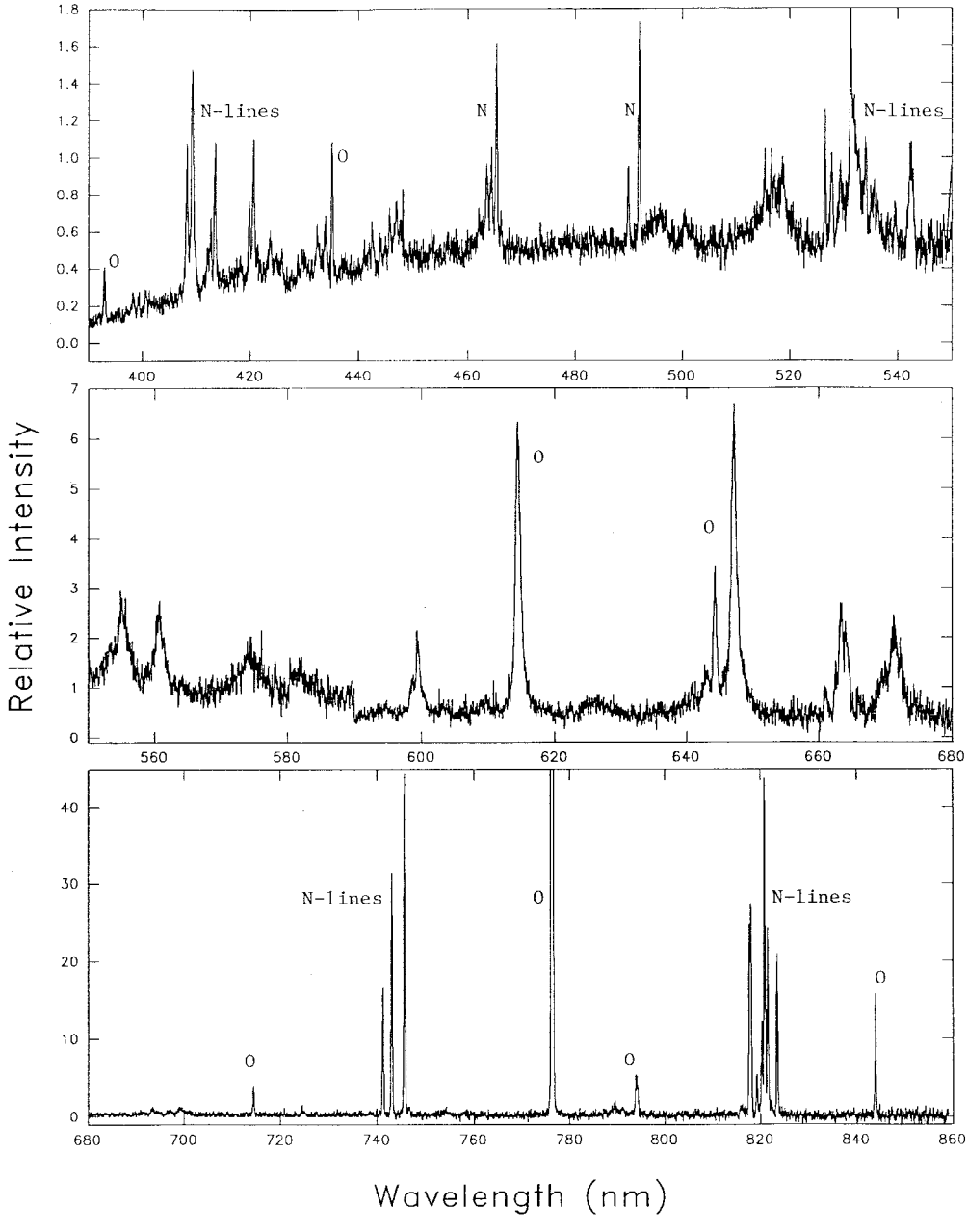

Fig. 2 Spectral radiation (390–860 nm) from the plenum area. The sharp lines are mostly a result of atomic oxygen and nitrogen emissions.

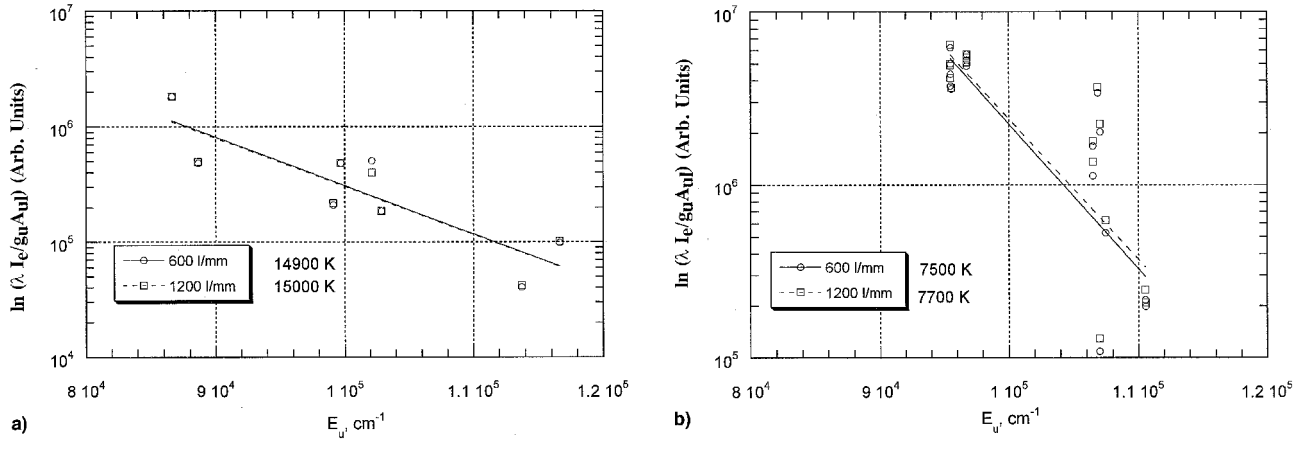

Fig. 3 Boltzmann plots of a) atomic oxygen and b) nitrogen emissions in case of high-enthalpy condition of arcjet.

Studies of individual plots of NO, N_2, and N_2^+ spectra, calculated using the NEQAIR code,[14] showed that the vibration–rotation transitions resulting from the $B\,^2\Sigma_u^+ - X\,^2\Sigma_g^+$ (or first negative) system of the N_2^+ molecule are more intense than the others in our current study conditions. We thus made high-resolution studies of the spectral bands involved in these transitions. Figure 4 shows these spectra in three different regions, showing vibrational bandheads of the $N_2^+(B - X)$ transitions for $\Delta v = 1$, 0, and -1. The bandheads are identified by comparing with the NEQAIR calculated spectra (see Fig. 5), and with the tabulated values.[18] A comparison of Figs. 4 and 5 shows that most of the $N_2^+(B - X)$ bandheads in the experimental spectra match very well with the theoretical spectra. The twin peaks around 389 nm could not be identified. These peaks have also been observed by Terrazas-Salinas et al.[9] in an arc-column spectral study, but we could not confirm the identification assigned by them.

To determine the molecular vibrational–rotational temperature, bandhead intensity ratios of the experimental spectra for the $\Delta v = 0$ and 1 transitions are compared with those of the NEQAIR plots at various temperatures (assuming vibrational and rotational temperatures to be same). These ratios are based on the intensity above the background continuum. Because of the low intensities of the bandheads, $\Delta v = -1$ transitions are not used for the vibrational-rotational temperature determination. The experimental intensity ratios obtained from Fig. 4a for the $\Delta v = 1$ transitions are tabulated in Table 4. Figure 6 shows plots of intensity ratios determined from NEQAIR-5 calculations as a function of temperature for the same $\Delta v = 1$ transitions. Temperatures are read from these plots, corresponding to each bandhead ratio given in Table 4. The determined temperatures are also shown in Table 4. The average temperature determined in this method for the $\Delta v = 1$ transi-

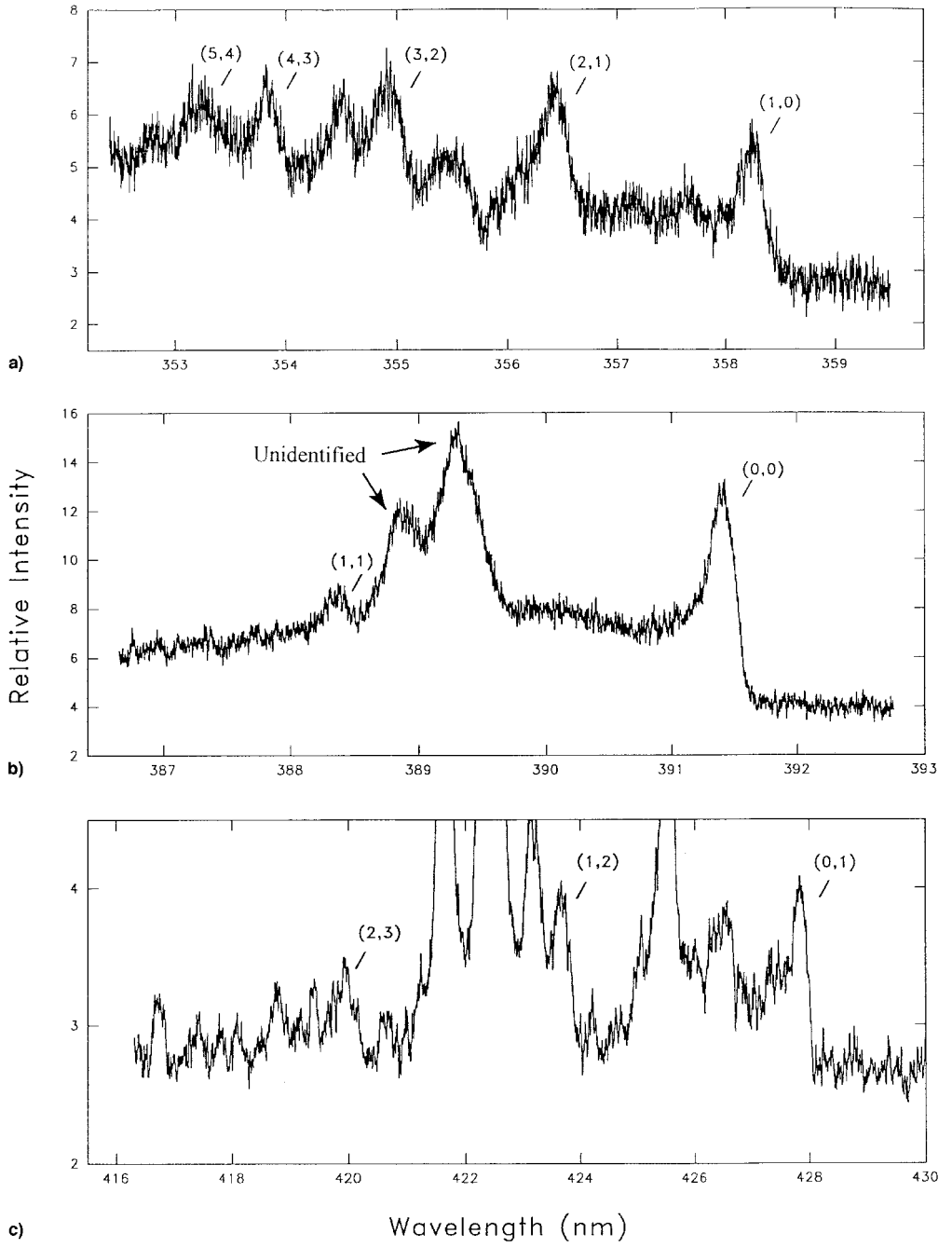

Fig. 4 High-resolution spectra in various spectral regions, identifying the vibrational bands of $N_2^+(B - X)$ transitions for Δv = a) 1, b) 0, and c) -1.

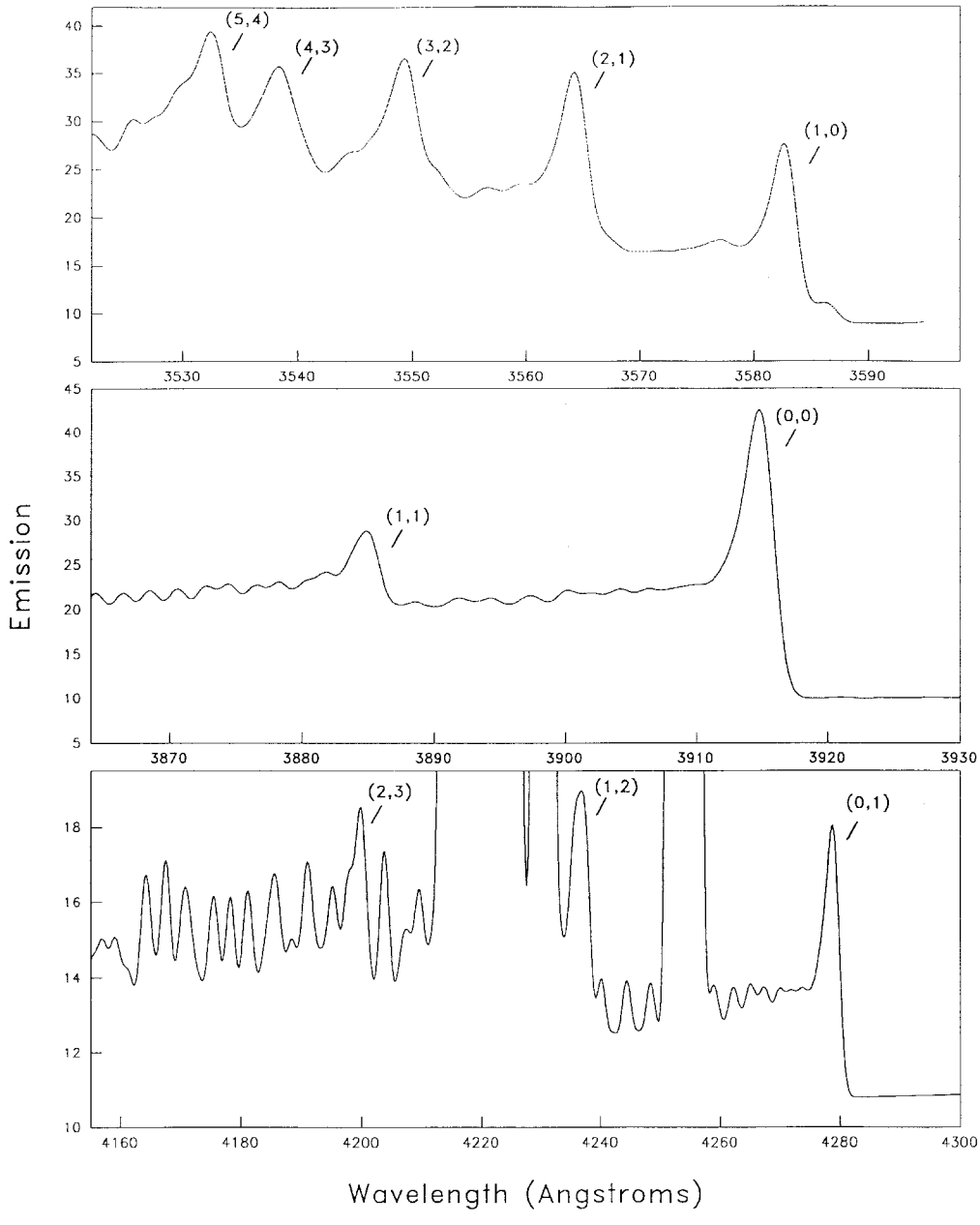

Fig. 5 Theoretical spectra resulting from combined N, N_2, and N_2^+ systems, plotted using the NEQAIR code, for the same spectral ranges as in Fig. 4. The temperature used in the code is 11,000 K.

Table 4 Vibrational bandheads and intensity ratios of $N_2^+(B - X)$ transitions

$v' - v''$	λ, A	$I_{(v'-v'')}$	$I_{(v'-v'')}/I_{(1-0)}$	T, K	T_{av}, K
1–0	3582.1	26	1.00	——	9800 ± 600
2–1	3563.9	37	1.40	10,500	——
3–2	3548.9	38	1.46	10,750	——
4–3	3538.3	36	1.28	9750	——
5–4	3532.6	35	1.17	8250	——

tions is about 9800 ± 600 K. The uncertainty in temperature in this case is taken as the standard error of the temperatures shown in Table 4. Using a similar comparison of ratios of bandhead intensities, for the (1,1) and (0,0) transitions, the temperature is found to be about 9000 ± 2000 K. However, if we take into consideration an assumed 10% uncertainty in the measured intensities, or 14% in the intensity ratio; the average vibrational–rotational temperature for all five intensity ratios is estimated to be 9700 ± 1200 K.

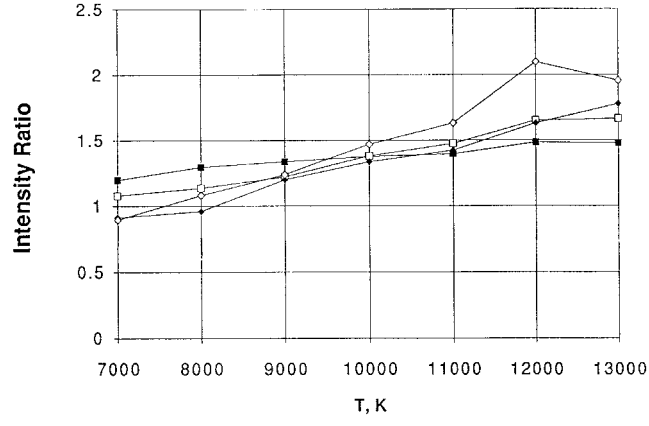

Fig. 6 Theoretical plots of intensity ratios ($I_{v',v''}/I_{1,0}$) of various vibrational bandheads of $N_2^+(B - X)$ transitions as a function of temperature. —■— (2,1)/(1,0); —□— (3,2)/(1,0); —◆— (4,3)/(1,0); —◇— (5,4)/(1,0).

IV. Conclusions

We have used an optical fiber to collect radiation from the plenum of an arcjet wind tunnel. The measurement zone is just downstream of the anode on which the arc attaches. Studying the spectra, we have determined the electronic excitation temperature from the Boltzmann plots of atomic oxygen and nitrogen emission lines. In the case of atomic oxygen, the temperature is found to be about 15,000 $\pm$ 3400 K, and that of nitrogen is found to be 7600 $\pm$ 1500 K. However, it is believed that the nitrogen results are unreliable. Determination of molecular vibrational–rotational temperature is made by comparing experimental and theoretical spectra of the N_2^+ molecular radiation. The temperature is estimated to be 9700 $\pm$ 1200 K, using an integrals ratio method. The difference in temperatures based on atomic lines and that from molecular bands may be explained on the basis that the atomic upper energy states are closely coupled with free electrons. Free electrons that do not exchange energy very quickly with the gas near the arc do not have sufficient time to relax as quickly as the molecules in the cooling flow downstream of the arc. Also, gradients in the flow may exist that result in more radiation from molecules in the cooler outer flow in the plenum.

The measurements can be improved by using a larger diameter fiber and a longer plenum. The radial distribution of the temperature can also be obtained by collecting light from different annular regions and using the Abel inversion technique.

Acknowledgments

We thank NASA/ASEE Summer Faculty Fellowship Program for providing support for the first two authors to work on this project. We also thank all NASA JSC and contract personnel of the arcjet facility, particularly J. D. Milhoan, Facility Manager, who provided us with necessary technical help. Thanks are also given to E. E. Whiting, of NASA Ames Research Center, for providing us with version five of the NEQAIR code. The comments and suggestions from the reviewers and the associate editor are greatly appreciated.

References

[1]Scott, C. D., "Effects of Thermochemistry, Nonequilibrium, and Surface Catalysis on the Design of Hypersonic Vehicles," edited by J. J. Bertin, R. Glowinski, and J. Periaux, *Hypersonics Volume I: Defining the Hypersonic Environment*, Birhäuser, Boston, MA, 1989, pp. 355–427.

[2]Scott, C. D., "Survey of Measurements of Flow Properties in Arcjets," *Journal of Thermophysics and Heat Transfer*, Vol. 7, No. 1, 1993, pp. 9–24.

[3]Arepalli, S., Yuen, E. H., and Scott, C. D., "Application of Laser Induced Fluorescence for Flow Diagnostics in Arc Jets," AIAA Paper 90-1763, June 1990.

[4]Scott, C. D., "Catalytic Recombination of Nitrogen and Oxygen on High-Temperature Reusable Surface Insulation," *Aerothermodynamics and Planetary Entry*, edited by A. L. Crosbie, Vol. 77, AIAA, Progress in Astronautics and Aeronautics, New York, 1981, pp. 192–212.

[5]Arepalli, S., "Optical Diagnostics for the Arcjet Facility at NASA/JSC," *Optical Diagnostics in Fluid and Thermal Flow*, edited by S. S. Cha and J. D. Trolinger, Vol. 2005, Society of Photo-Optical Instrumentation Engineers, 1993, pp. 2–13.

[6]Blackwell, H. E., Arepalli, S., Yuen, E. H., and Scott, C. D., "Analysis of N_2 Shock Layer Emission and the Measurement of Arcjet Temperatures," AIAA Paper 90-1736, June 1990.

[7]Blackwell, H. E., Wierum, F. A., and Scott, C. D., "Spectral Determination of Nitrogen Vibrational Temperatures," AIAA Paper 87-1532, June 1987.

[8]Babikian, D. S., Gopaul, N. K. J. M., and Park, C., "Measurement and Analysis of Nitric Oxide Radiation in Arc-Jet Flow," AIAA Paper 93-2800, July 1993.

[9]Terrazas-Salinas, I., Park, C., Strawa, A. W., Gopaul, N. K. J. M., and Taunk, J. S., "Spectral Measurements in the Arc Column of an Arc-Jet Wind Tunnel," AIAA Paper 94-2595, June 1994.

[10]Bade, W. L., and Yos, J. M., "The NATA Code: User's Manual," NASA CR-141743, 1976.

[11]Rob, M. A., Mack, L. H., Arepalli, S., and Scott, C. D., "Spectral Measurements in the Plenum of an Arcjet Wind Tunnel," AIAA Paper 95-2126, June 1995.

[12]*M.I.T. Wavelength Tables*, MIT Press, Cambridge, MA, 1963.

[13]Wiese, W. L., Smith, M. W., and Glennon, B. M., *Atomic Transition Probabilities, Vol.1 Hydrogen Through Neon*, NSRDS—NBS 4, 1966.

[14]Park, C., *Nonequilibrium Air Radiation (NEQAIR) Program: User's Manual*, NASA TM-86707, 1985.

[15]Wiese, W. L., "Spectroscopic Diagnostics of Low Temperature Plasmas: Techniques and Required Data," *Spectrochemica Acta*, Vol. 46B, Nos. 6/7, 1991, pp. 831–841.

[16]Griem, H. R., *Plasma Spectroscopy*, McGraw–Hill, New York, 1964, p. 307.

[17]Marr, G. V., *Plasma Spectroscopy*, Elsevier, New York, 1968, p. 288.

[18]Lofthus, A., and Krupenie, P. H., "The Spectrum of Molecular Nitrogen," *Journal of Physical Chemistry*, Vol. 6, No. 1, 1977.